

Some multi time-scale aspects in shock wave/boundary layer interaction.

JF. Debieve and P. Dupont.

Université de Provence. Lab. IUSTI, UMR CNRS 6595.
5 rue Enrico Fermi, 13453 Marseille Cedex 13, France

ABSTRACT

The interaction of an oblique shock wave impinging on a turbulent boundary layer at Mach number 2.3 is experimentally investigated. Characteristic time and length scales of the unsteady reflected shock and also in the downstream interaction region are obtained and compared with already existing results obtained in compression ramp experiments as well as in subsonic detached flows. Dimensionless characteristic frequencies are highlighted to characterise low frequency shock unsteadiness as well as the different large scales which develop inside the initial part of the interaction. The possibility to describe the spatial development of the large scales inside the interaction zone using a mixing layer scheme including compressibility effects is tested for a wide range of Mach numbers, shock intensities and geometrical configurations. Moreover, strong evidence of statistical link between low frequency shock movements and the downstream interaction is given. Finally, the downstream evolution of the structures shed into the boundary layer is characterised and shows features specific of our configuration.

INTRODUCTION.

We present experimental results obtained in the low turbulence supersonic wind tunnel at the *Institut Universitaire des Systèmes Thermiques Industriels*. A turbulent boundary layer at Mach number of 2.3 impinged by an oblique shock wave with various intensities is studied. Strong unsteadiness is developed in the separated zone. It involves different frequency ranges which can extend over several orders of magnitude. Each zone is associated with typical temporal scales [1], which can be superimposed. This results in a multi time-scale problem which generates different turbulent structures where compressibility effects can be not negligible.

FIRST CHARACTERISATION OF THE FLOW.

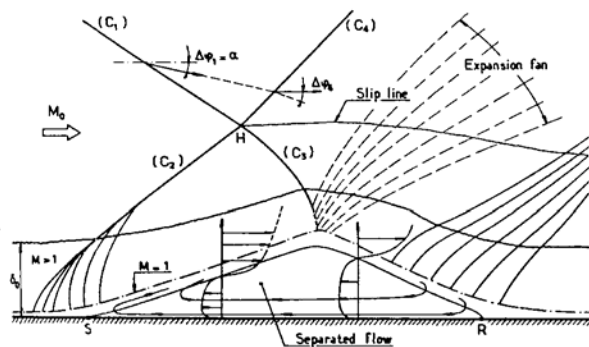


Figure 1: Schematic representation of shock reflection with a boundary layer separation (from AGARDograph n°280 Delery Marvin, [7]).

The flow as sketched in Figure 1, can be qualitatively separated in four zones:

1) an incoming turbulent boundary layer which is impinged by a steady incident shock. In this incoming flow, no evidence of energetically significant low frequencies was observed for the wall pressure. Turbulence presents an usual spectral content: in previous work, measurements carried out in the flow itself by Constant Current Anemometer have provided similar information on spectral properties of the incoming boundary layer: longitudinal velocity, momentum and temperature spectra were measured inside the boundary layer. They showed a maximum of energy for $f \delta / U_0 \sim 0.6$ with a corresponding frequency $f \sim 30 \text{kHz}$.

2) an unsteady reflected shock which can be described as a shock sheet oscillating at low frequency, around a few hundreds Hz, two orders of magnitude less than turbulence in the incoming boundary layer. The corresponding Strouhal number $S_L = fL / U \sim 0.03$, Figure 2. L is defined as the distance at the wall between the incident and reflected shocks. For this we use an extrapolation at the wall of these shocks. $X^* = (x - x_0) / L$ is a dimensionless longitudinal coordinate ($X^*=0$ on the reflected shock, and the interaction extends up to 1).

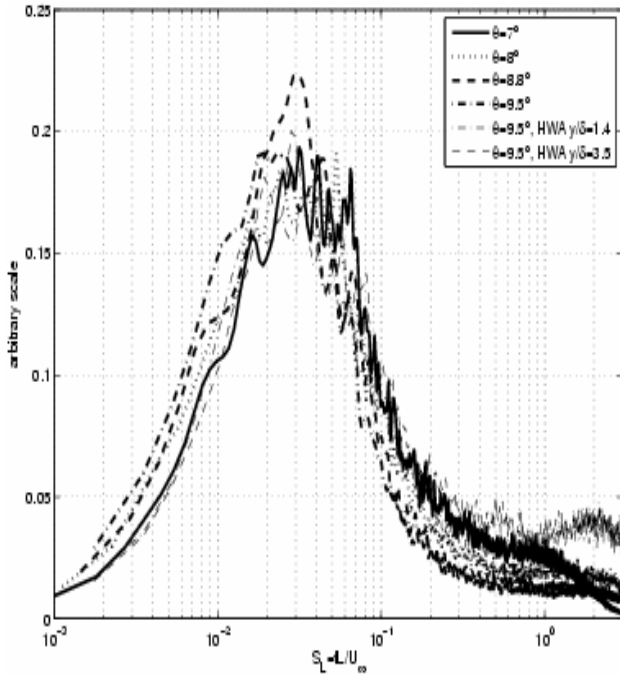


Figure 2: Pressure and hot wire signal power Spectral Density on the reflected shock, ($X^*=0$). Normalised frequencies $S_L = fL/U_\infty$.

Similar values of this Strouhal appear in other configurations as compression ramps, [2]. The space amplitude of the reflected shock motion increases with the shock intensity and vanishes far from the wall. In the vicinity of the foot of the shock an important increase of the turbulence intensity level is produced. The turbulence level of pressure fluctuation can reach, in order of magnitude, the half of the mean pressure step through the shock, Figure 3. This bump of turbulence on the shock can be associated with a spatial intermittency of the reflected shock position.

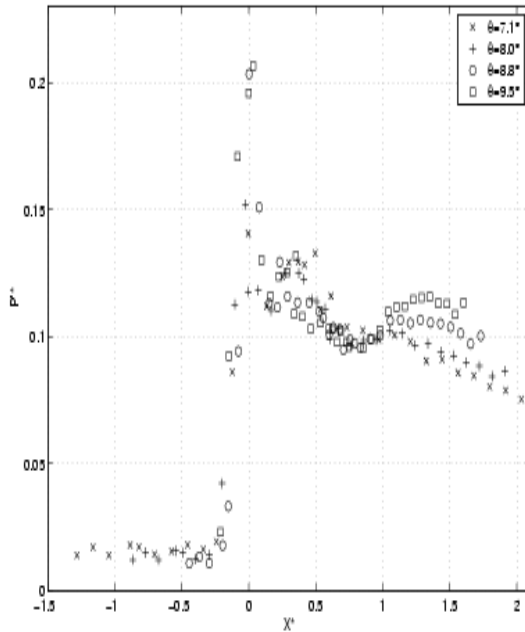


Figure 3: Dimensionless rms. wall pressure fluctuations $p^* = \sqrt{p^2 / (p_2 - p_1)}$ for $7^\circ < \theta < 9.5^\circ$

3) In the detached zone, a 'mixing layer' is developing and reattaches near the end of the interaction. Associated to this separation, medium time scales, (a few KHz) are found as in subsonic separations. In our case, there is a strong acceleration, downstream of the expansion fan in the middle of the interaction zone. Superimposed on these scales, frequencies of one order of magnitude lower (in the same range as the characteristic frequencies associated with the reflected shock) have been identified in the second part of the interaction zone. So, in this zone, we have a multi time-scale problem: high frequencies of same order as in a classical turbulent boundary layer, medium time scales as in a mixing layer, and very low frequencies, of the same order as for the moving shock.

4) A relaxation zone follows, located downstream with a remainder of the previous medium frequencies.

INTERACTION ZONE.

Here, attention is focused on the multi-frequency scale aspect in the separated zone downstream of the reflected shock.

In our case, only a little part of the turbulence level downstream the reflected shock can be explained using rapid distortion theory. The linear amplification through the shock is not sufficient. Another possible explanation consists in describing the spatial development of the scales inside the interaction zone using a mixing layer scheme including compressibility effects. It is tested for other Mach number ranges (including subsonic), other shock intensities and other geometrical configurations.

The PSD's, in the $fE(f)$ representations, are found to reach a maximum level in a medium frequency range ($0.3 < S_L < 2$). The evolution of these dominant frequencies along the interaction for the different shock intensities are summarised in Figure 4. An usual interpretation in subsonic recirculating flows consists in associating such frequencies with the large convective scales of the mixing layer which develops from the separation point [3, 4]. In such a case, because of the mixing process, the mean distance between large structures increases linearly as they are convected downstream, (likewise for S_L^{-1}). Such a behaviour is observed at the beginning of the interaction ($X^* < 0.5$), but is followed by a constant level in the second half of the recirculating bubble; this saturation is associated with some vortex shedding downstream.

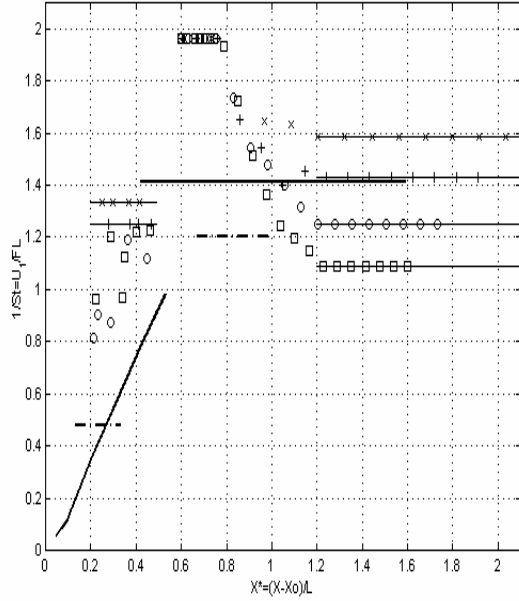


Figure 4: Longitudinal evolution of Strouhal number S_L^{-1}

- subsonic detached flow [Cherry et al (1984)]; - - $-M=1.5$ ramp flow [Thomas et al. (1994)]; present experiments (x) $\theta=7^\circ$, (+) $\theta=8^\circ$, (o) $\theta=8.8^\circ$ and (\square) $\theta=9.5^\circ$.

The centre of the detached zone, ($0.5 < X^* < 0.8$) presents a behaviour similar to the subsonic case, with a nearly constant shedding frequency: around $S_L \sim 0.5$ for the whole range of shock intensities, but with a level significantly different from the subsonic one.

The kinematics of these scales has also been characterised by two-point measurements. The phase velocity associated with the dominant frequency is presented in Figure 5, for the different shock intensities. For all cases, in the region $0.2 < X^* < 0.8$, where the spatial behaviour of the dominant frequency is similar to the subsonic case, a mean value of the phase velocity of approximately 150ms^{-1} is obtained.

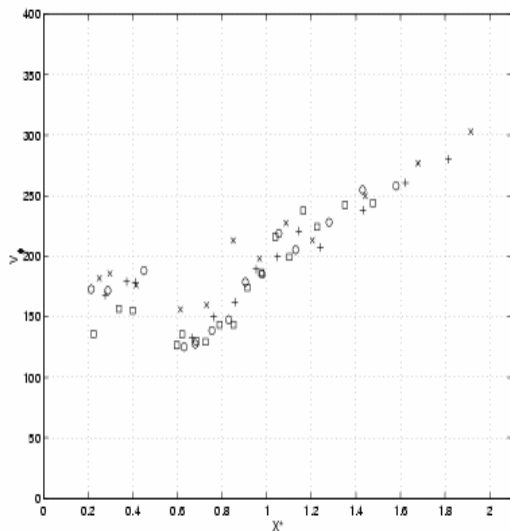


Figure 5: Phase velocities V_ϕ , (ms^{-1}) of the characteristic

frequency along the interaction.

We have remarked in Figure 4 various evolutions of the Strouhal S_L based on the length L : mainly an important difference which exists on the extrema or ‘shedding’ levels reached in the incompressible case and in the centre part of the shock separation. Additional effects can alter the layer behaviour; we can suspect a more or less important effect of asymmetrical layer or confinement according to the intensity of the back-flow. In connection with this parameter, the compressibility effect on the Strouhal number can also be analysed, at least in the initial part of the interaction. Using mixing layer approximations, we can write:

$$S_L \sim (S_{tr}/\delta') \cdot (U_c/U_\infty) \cdot X^{*-1}$$

where $S_{tr} = f\delta/U_c$ is the classical Strouhal number for mixing layer and δ' the spreading rate. The first term of the right hand side is nearly constant, [5]. Thus:

$$S_L \sim \text{cst} \cdot (U_c/U_\infty) \cdot X^{*-1} \quad (1)$$

where U_c is the convection celerity of the structures. For moderate convective Mach number U_c/U_∞ depend on the direct and counter velocity ratio ‘ r ’, and also on the associated density ratio ‘ s ’. In incompressible mixing layer or using isentropic approximation for moderate convective Mach number, we can write the classical dependency:

$$\frac{U_c}{U_\infty} = \frac{1 + r\sqrt{s}}{1 + \sqrt{s}}$$

Using this procedure, the comparison with direct subsonic measurements of S_L vs. X^* performed by Cherry et al. ($S_L = 0.5X^{*-1}$) seem in satisfactory agreement. But, in our case of supersonic separation, the convective Mach number can rather reach a value of 1, and the estimation of U_c using isentropic model may be dangerous: by this way the convective velocity will overestimate by around 70% a direct estimation of U_c . But, using the experimental phase celerity measured previously $U_c/U_\infty = 0.3$, and equation $n^{\circ}1$, we obtain $S_L \sim 0.34X^{*-1}$, which is consistent with our results. So, such a slope variation, explained by a compressibility effect, leads to the Strouhal levels reached in the middle of the separation, Figure 4.

Downstream of these mixing and shedding zones, the dimensionless frequency evolves continuously in the region $0.8 < X^* < 1.2$, and in a way different from the subsonic case, to reach different nearly constant level depending on the shock intensity in the beginning of the relaxation, Figure 4. The typical evolution, in our configuration, of the Strouhal number in the zone $0.8 < X^* < 1.2$, is not observed in the experiments for the compression ramp where the downstream flow may have very different features.

In parallel, strong increase of the phase velocity is observed in the region $0.8 < X^* < 1.2$, where the dominant frequencies have also been found to increase, Figure 5. This region starts at the expansion fan associated with the reflection of the incident shock.

STATISTICAL LINKS WITH THE REFLECTED SHOCK.

In addition some low frequency events ($S_L \sim 0.04$), close to the frequencies of the reflected shock motions, have also been identified in the second part of the interaction; a secondary small bump on spectral power repartition, appears in the Strouhal range [.001-1], Fig. 6.

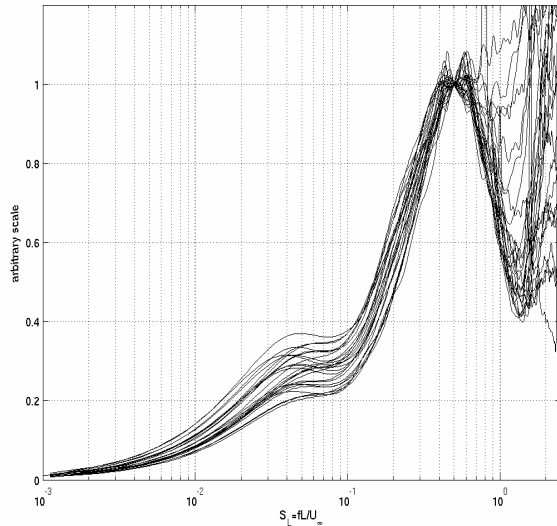


Figure 6: Pressure Power Spectral Density inside the interaction zone for the various shock intensities ($7.1 < \theta < 9.5^\circ$) in the region $0.6 < X^* < 0.77$. Normalised frequencies fL/U_∞ .

They contribute up to 30% of the total energy of the measured pressure fluctuations, (without taking into account the apparatus cut off). Moreover, these low frequencies are found in quasi linear dependence with reflected shock motions: the coherence function between the pressure at the mean reflected shock position and the pressure in the second part of the separation keeps a significant value, close to 1, for the low frequency range, Figure 7. In this range, the same as for the shock oscillation, the phase relation will show a phase shift near π between the pressure signals at the reflected shock and in the separation zone. Such a behaviour has been already found by Thomas et al. [6], in a compression ramp flow. Moreover a negative value of the slope of this phase relation gives the indication of a propagation in a backwards direction, at least for the strongest interaction, (9.5° case). To confirm this tendency, we rather used the two points correlation function and the associated time delay. The correlation has been estimated between a point on the mean shock and a location in the separation (solid line) or downstream of the reattachment point (dashed line), Figure 8. The data has been low-pass filtered according to the shock frequency range. The resulting correlation is negative, (phase π); but more interestingly we can also notice a shift of the time delay associated to its optimum. The time delay is clearly positive in the separation zone ($X^* < 1$), and negative elsewhere; that confirms, in the separation zone, the existence of a backward influence in the upstream direction, Figure 9. This behaviour for low frequencies does not persist downstream of the reattachment point ($X^* > 1$) where the sign of the time delay is inverted. In the separated zone

the value of this backward celerity is larger than the mean counter flow velocity and less than the sound velocity. This behaviour is less clear for the weaker interaction for the 8° deflection case. Nevertheless, while the exact mechanism which links both zones has not yet been identified, it is clear that shock motions at low frequency are related to low frequency events inside the separated zone.

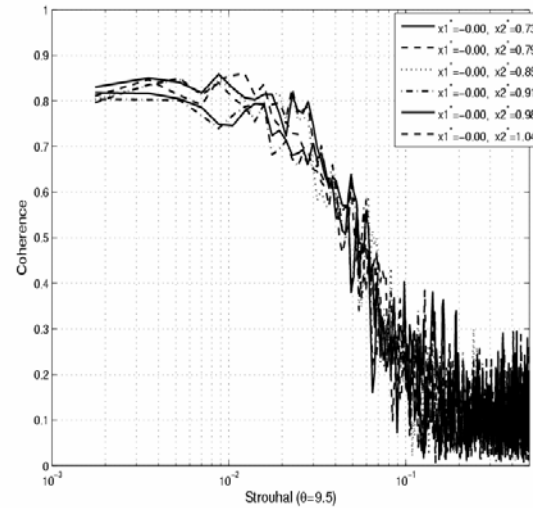


Figure 7: Coherence function between wall pressure signals recorded in the vicinity of the reflected shock and near the reattachment region, $\theta = 9.5^\circ$.

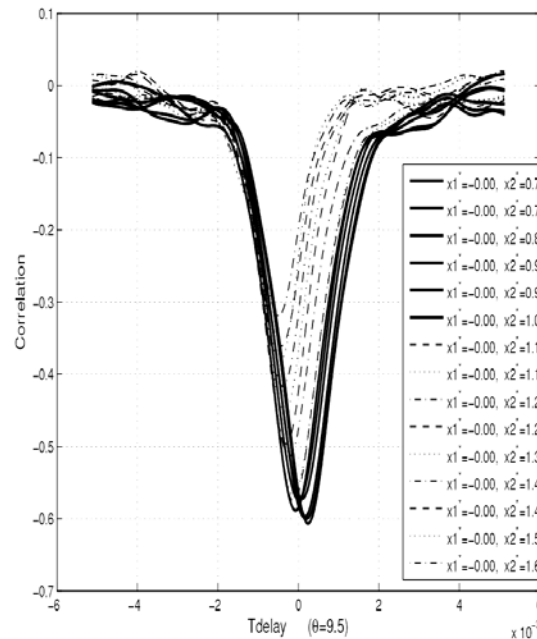


Figure 8: Correlation between the shock and a location in the separation (full line) or downstream of the reattachment point (dashed line);

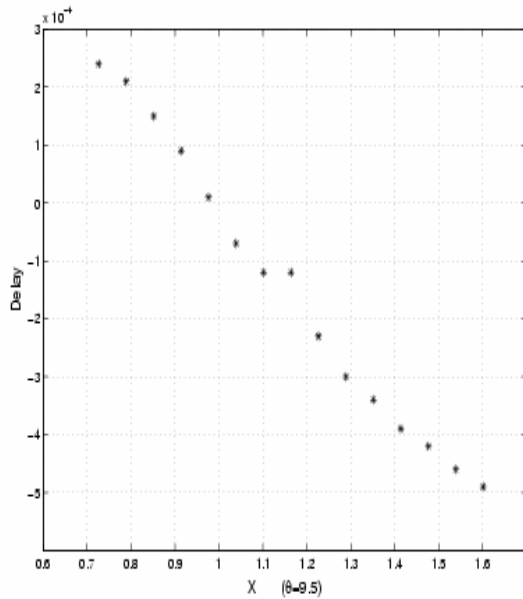


Figure 9: Time delay associated with the optimum of the correlation.

CONCLUSION.

Only one dimensionless characteristic frequency has been used to characterise the low frequency shock unsteadiness as well as the various large scales which develop inside the initial part of the interaction. As a first step, it seems that a length scale such as L or the length scale of the detached zone used in subsonic flow, seems appropriate to define a Strouhal in shock induced separation, for a wide range of configurations. Nevertheless, we need some additional compressibility correction, to explain the particular turbulence behaviour, as in the mixing part of the interaction. The possibility of a mechanism corresponding to the backward action at low frequency, from the detached zone on the moving reflected shock, has to be elucidated.

ACKNOWLEDGEMENTS.

Part of this work was carried out with the support of the Research Pole ATAC. CNES/ONERA and 'Programme de Recherche Aéronautique sur le Supersonique, Ministère de la Recherche.

BIBLIOGRAPHY.

[1] Haddad C., *Instationnarités, mouvements d'onde de choc et tourbillons à grandes échelles dans une interaction onde de choc/couche limite avec décollement*, Université de Provence Aix-Marseille I, Thèse de Doctorat 2005

[2] Erenkil M.E., Dolling D.S., *Unsteady wave structure near separation in a Mach 5 compression ramp interaction*, AIAA Journal, Vol.29, N°5, pp. 728-735, 1991.

[3] Kiya M., Sasaki K., *Unsteady wave structure near separation in a Mach 5 compression ramp interaction*, J.

Fluid Mech., Vol. 137, pp. 83-113, 1983.

[4] Cherry N.J., Hillier R., Latour M.E.M., *Unsteady measurements in a separated and reattaching flow*, J. Fluid Mech., Vol. 144, pp. 13-46, 1984.

[5] P. Dupont, C. Haddad, J.F. Debiève . *Space and Time Organization in a Shock induced Separated Boundary Layer*. To be publish in J. Fluid Mech. 2005.

[6] Thomas F.O., Putman C.M., CHU H.C., *On the mechanism of unsteady shock oscillation in shock wave/turbulent boundary layer interaction*, Experiments in Fluids, Vol.18, pp. 69-81, 1994.

[7] Delery J, Marvin JG, *Shock wave/boundary layer intractions*. AGARDograph n°280, NATO,1986.